Self-Assembly

International Edition: DOI: 10.1002/anie.201807937
German Edition: DOI: 10.1002/ange.201807937

Dissipative Self-Assembly of Photoluminescent Silicon Nanocrystals

*Raphael K. Grötsch[+], Arzu Angı[+], Yonatan G. Mideksa, Caren Wanzke, Marta Tena-Solsona, Matthias J. Feige, Bernhard Rieger, and Job Boekhoven**

Abstract: *Solutions of silicon nanocrystals (SiNCs) are used in a diverse range of applications because of their tunable photoluminescence, biocompatibility, and the abundance of Si. In dissipative supramolecular materials, self-assembly of molecules or nanoparticles is driven by a chemical reaction network that irreversible consumes fuel. The properties of the emerging structures are controlled by the kinetics of the underlying chemical reaction network. Herein, we demonstrate the dissipative self-assembly of photoluminescent SiNCs driven by a chemical fuel. A chemical reaction induces self-assembly of the water-soluble SiNCs. However, the assemblies are transient, and when the chemical reaction network runs out of fuel, the SiNCs disassemble. The lifetime of the assemblies is controlled by the amount of fuel added. As an application of the transient supramolecular material, we demonstrate that the platform can be used to control the delayed uptake of the nanocrystals by mammalian cells.*

Silicon nanocrystals (SiNCs) have garnered significant attention[1] for their unique properties, which include size-dependent photoluminescence,[2] low-toxicity,[3] and biocompatibility.[4,5] Moreover, the elemental abundance of silicon favors the applications in sensors,[6] LEDs,[7] solar cells,[8] and bio-imaging.[9,10] The surface chemistry of SiNCs plays a critical role in these applications because it can alter the nanocrystal's natural properties.[11] Thus properties such as cytotoxicity,[12] photoluminescent emission quantum yield,[13] or emission wavelength,[14] can be tuned through functionalization of the SiNCs' surface. Strategies to modify the surface chemistry of the SiNCs rely on the formation of stable, covalent bonds. The static nature of these bonds does not allow for dynamic material properties that evolve or that adapt to environmental changes.

In contrast, dissipative supramolecular materials are intrinsically dynamic, and their function can be controlled over space and time.[15] For these materials, the self-assembly of molecules is coupled to (photo)chemical reaction networks. In these chemical reaction networks, an activation reaction activates a precursor, which enables the precursor to undergo self-assembly. The reaction can only occur at the expense of a source of energy, typically a photon or a chemical fuel, and is irreversible. That is, the activation reaction "burns" a source of energy to activate a precursor for self-assembly. The activated product can then self-assemble to form a supramolecular material. However, the product is metastable and spontaneously deactivates into the original precursor via the deactivation reaction. The dissipative self-assembly implies that the supramolecular material is dynamic and forms in response to energy. Man-made examples of dissipative self-assembly include the ATP-fueled assembly of amphiphiles into temporary nanoreactors,[16] the formation of transient self-healing hydrogels driven by the hydrolysis of methylating agents,[17] the carbodiimide-driven formation of colloids that can deliver hydrophobic agents,[18] among others.[19,20] In the context of the dissipative assembly of nanoparticles, researchers have described the light-driven self-assembly of silver and gold nanoparticles into self-erasing inks,[21] and the dynamic pH controlled clustering of gold nanoparticles.[22] Another example used methylating agents to drive the assembly of colloids.[20]

Herein, we describe a new chemical reaction network that drives the dissipative self-assembly of SiNCs (Figure 1 a). We show that the emerging clusters of SiNCs change size predictably over time and that the emerging materials can be re-used in multiple cycles. We use the evolving size of the SiNC clusters to delay the uptake of the SiNCs by mammalian fibroblasts-like cells. The combined experiments open a platform that could deliver therapeutics with a delayed and regulated uptake kinetics.

We functionalized SiNCs with 5-hexenoic acid to make them water-soluble (the precursor in Figure 1 a). An acid-titration experiment revealed their pKa to be approximately 6.9 (Figure SI1 in the Supporting Information). The SiNCs were dissolved in a buffer at a final surface-bound carboxylic acid concentration of 5 mM. The buffer we used was a 200 mM 2-(*N*-morpholino)ethanesulfonic acid (MES) buffer with 100 mM *N*-hydroxysuccinimide (NHS) at pH 6.5 in water. At this pH, more than half of the carboxylic groups on the SiNCs were deprotonated. As a result, the electrostatic

[*] R. K. Grötsch,[+] C. Wanzke, Dr. M. Tena-Solsona, Prof. Dr. J. Boekhoven
Department of Chemistry, Technische Universität München
Lichtenbergstrasse 4, 85748 Garching (Germany)
E-mail: job.boekhoven@tum.de
A. Angı,[+] Prof. Dr. B. Rieger
WACKER-Lehrstuhl für Makromolekulare Chemie
Technische Universität München
Lichtenbergstrasse 4, 85748 Garching (Germany)
and
Catalysis Research Center
Ernst-Otto-Fischer-Strasse 1, 85748 Garching (Germany)
Y. G. Mideksa, Prof. Dr. M. J. Feige
Center for Integrated Protein Science at the Department of Chemistry, Technische Universität München
Lichtenbergstrasse 4, 85748 Garching (Germany)
R. K. Grötsch,[+] Y. G. Mideksa, C. Wanzke, Dr. M. Tena-Solsona, Prof. Dr. M. J. Feige, Prof. Dr. J. Boekhoven
Institute for Advanced Study, Technische Universität München
Lichtenbergstrasse 2a, 85748 Garching (Germany)
[+] These authors contributed equally to this work.
Supporting information and the ORCID identification number(s) for the author(s) of this article can be found under: https://doi.org/10.1002/anie.201807937.

 © 2018 Wiley-VCH Verlag GmbH & Co. KGaA, Weinheim

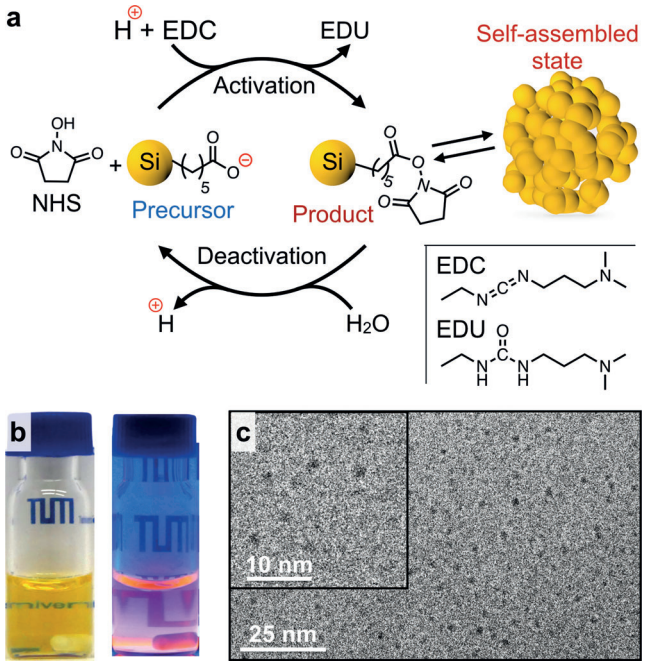

Figure 1. a) Schematic representation of the chemical reaction network. Carboxylate surface groups on the SiNCs react with EDC and NHS to form a transient NHS ester. The loss of surface charges induced the temporary self-assembly of SiNCs. b) Photographs of a solution of the precursor in MES buffer under visible (left) and UV (365 nm, right) light. c) Cryo-TEM images of the precursor solution.

stabilization achieved by these charges made the SiNCs well-soluble in the buffer. Indeed, dissolution of the SiNCs in the buffer yielded a yellow transparent colloidal solution (Figure 1b). Under UV irradiation the yellow solution emitted red light, strongly indicating that the SiNCs maintained their intrinsic photoluminescence. The emission was further verified in a spectrophotometer, which showed a photoluminescent emission maximum at 681 nm when irradiated with 365 nm UV light (Figure SI2). We determined the hydrodynamic diameter of the SiNCs to be (5.5 ± 1.1) nm by dynamic light scattering (Table SI1). Cryogenic transmission electron microscopy (cryo-TEM) corroborated the successful synthesis of the SiNCs and their homogeneous dissolution. From the micrographs, we determined their diameter to be (3.6 ± 0.5) nm (Figure 1c, Figure SI3b). Finally, UV/Vis spectra of the SiNCs showed absorption at wavelengths shorter than 400 nm (Figure SI4).

The carboxylic acid functionalized SiNCs served as the precursors in the chemical reaction network we introduce herein (Figure 1a). In the activation reaction, the carboxylate groups on the SiNC surface were converted into the corresponding NHS-esters by the irreversible consumption of 1-ethyl-3-(3-dimethylaminopropyl) carbodiimide (EDC). In the deactivation reaction, the NHS esters hydrolyzed back to their initial carboxylate state. The cycle could only operate for as long as EDC was present because the activation irreversibly consumed EDC. Moreover, the loss of electrostatic stabilization upon the conversion of the precursor induced assembly of the SiNCs into clusters. Taken together, the irreversible consumption of EDC induced the transient assembly of the SiNCs.

We studied the kinetics of the aforementioned reaction network. The SiNCs solution was fueled with a 7 mM solution of EDC, and the evolution of the concentration of EDC was monitored via high-pressure liquid chromatography (HPLC, Figure 2a). The concentration of EDC decreased to less than

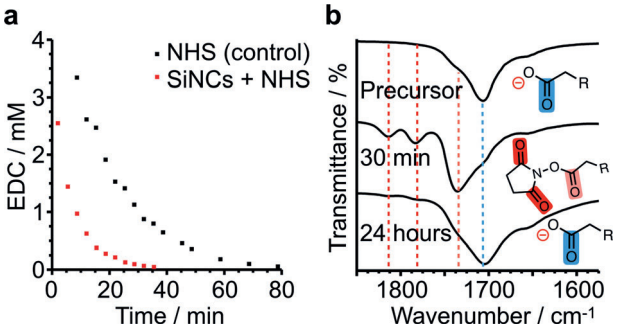

Figure 2. a) The EDC concentration as a function of time. The red markers correspond to the addition of 7 mM EDC to a solution of SiNCs in MES-buffer (200 mM) and NHS (100 mM), the black markers show the same experiment without the SiNCs as a control. b) FTIR spectra of the precursor SiNCs; 30 min and 24 h after addition of 7 mM EDC. Dashed lines from left to right: 1814, 1784, 1738, 1706 cm^{-1} (R = -$(CH_2)_4$-SiNC).

3 mM within the first minute, after which it further decayed exponentially. No substantial amount of EDC was detected after 35 min. The initial rapid decay was likely a result of a reaction of EDC with NHS.[23] This hypothesis was further corroborated by a similar rapid decrease in the EDC concentration in a control experiment without the SiNCs (Figure 2a). The EDC decay rate was higher in the presence of SiNCs than in the control reaction. This accelerated decay served as a good indicator of the reaction between the carbodiimide and the carboxylate surface groups of SiNCs.

We monitored the surface groups of the SiNCs in response to EDC by Fourier-transform infrared (FTIR) spectroscopy (Figure 2b, see Figure SI5 for full spectra). Before the addition of EDC, the spectrum of the SiNCs showed a C=O band at 1706 cm^{-1}, which corresponds to the carboxylic acid groups.[24,25] Upon the addition of 7 mM EDC, the peak at 1706 cm^{-1} weakened to a small shoulder and three new peaks arose at 1814 cm^{-1}, 1784 cm^{-1} and 1738 cm^{-1}, which correspond to ν_s(C=O, NHS ester), ν_s(C=O NHS imide), and to ν_s(C=O NHS-imide), respectively. Importantly, 24 h after the addition of EDC, the NHS-ester peaks mostly disappeared, whereas the carboxylic acid peak at 1706 cm^{-1} recovered (Figure 2b). This result is a good indication that the NHS ester is transient and hydrolyzes to the original precursor. The combined results demonstrate that the carboxylic acids on the SiNCs' surface were transiently converted into their corresponding NHS ester at the expense of EDC.

The initially yellow clear solution became turbid upon the addition of EDC. Moreover, the turbid solution became transparent over the course of hours, pointing to an assembly and disassembly process of the SiNCs. We used time-lapse photography to follow the changes in turbidity over time

 © 2018 Wiley-VCH Verlag GmbH & Co. KGaA, Weinheim

These are not the final page numbers!

(Figure 3a). An EDC concentration of at least 6.5 mM was required to induce a noticeable increase in turbidity. When the EDC concentration was 6.5 mM, the increase in turbidity persisted for more than 4 h. Moreover, we observed that, with increasing EDC concentration, the samples remained turbid longer. For example, with 12.5 mM EDC, which corresponds to a 2.5-fold excess of fuel over the surface-bound carboxylates, the turbidity persisted approximately 17 h. When a 20-fold excess of fuel was added, the solutions remained turbid for longer than 2 days (Figure SI6).

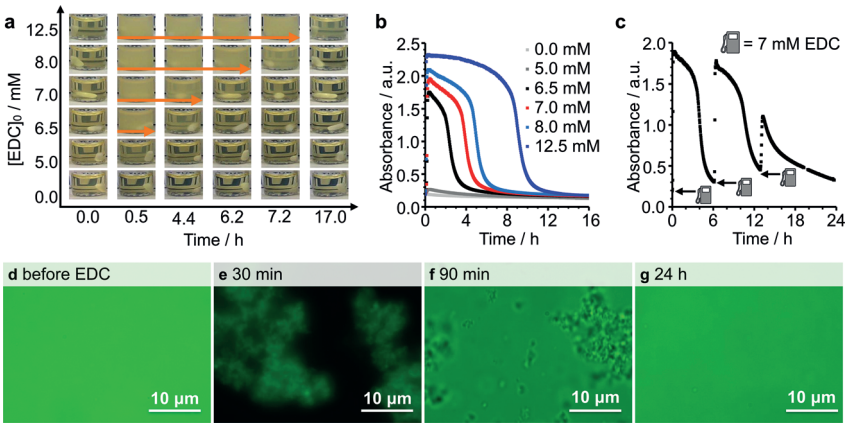

Figure 3. a) Photographs of SiNC solutions with different initial EDC concentrations over time; each column represents a different time point. b) Absorbance at 500 nm over time as a quantification of turbidity induced by the addition of different concentrations of EDC (0.0, 5.0, 6.5, 7.0, 8.0, and 12.5 mM). c) Three consecutive additions of 7 mM EDC to the same SiNC solution. Turbidity was monitored via UV/Vis spectrophotometry (absorbance at 500 nm). d)–g) Fluorescent micrographs acquired before (d) and 30 min (e), 90 min (f) and, 24 h (g) after the addition of 7 mM EDC. The intrinsic fluorescence of the SiNCs was measured.

We quantified the transient turbidity by measuring the absorbance at 500 nm in a UV/Vis spectrophotometer. When EDC was added to the samples, the turbidity increased in the first 30 min to a maximum, then decreased to its original level (Figure 3b). To quantify the lifetime of the increased turbidity, we set an arbitrary absorbance threshold at 0.27 absorbance units. Above this threshold, the sample was considered turbid; below the threshold, it was considered transparent. We found that the lifetime of the turbidity increased linearly with increasing EDC concentration between 6.5 to 12.5 mM (Figure SI7).

We used the intrinsic photoluminescence of the SiNCs in combination with fluorescence microscopy to study the nature of the turbidity in greater detail. Before the addition of EDC, fluorescence microscopy revealed a homogeneous fluorescent solution without evidence of assemblies. In contrast, 30 min after the addition of 7 mM EDC, we observed bright fluorescent clusters of tens of micrometers, whereas the surrounding solution showed no fluorescent emission (Figure 3d,e). From the lack of fluorescence in the surrounding solution, we concluded that most of the SiNCs had been incorporated into the clusters. After 90 min, we observed smaller clusters and the surrounding solution started to emit light again (Figure 3f). These observations point toward the disassembly of the clusters into the SiNCs. After 24 h, we observed a homogeneous photoluminescent solution, reminiscent of the solution shown in the micrographs collected before the addition of EDC (Figure 3g). Moreover, cryo-TEM images of SiNC solutions after the reaction cycle revealed a size distribution of SiNCs ($d = 3.6 \pm 0.7$ nm) similar to that before the addition of EDC (Figure 1c, Figure SI3). Unfortunately, cryo-TEM on the samples during the cycle proved challenging probably because of the size of the clusters. Instead, we used confocal microscopy and found clusters of the particles of tens of microns in all three dimensions (Figure SI8).

The possibility of inducing transient assembly of the SiNCs in consecutive cycles was also tested. The first reaction cycle was initiated with the addition of 7 mM EDC. After the solution had lost its turbidity, the next cycle was started by addition of a new batch of 7 mM EDC. The turbidity measurements showed that the cycles could be repeated as many as three times. However, the third cycle showed signs of fatigue, that is, the maximum turbidity the sample reached was only 59% of the value compared to the first cycle. All three cycles showed lifetimes of approximately 6.2 h (Figure 3c). Two possible reasons could explain the fatigue: The reaction between the carboxylic acids and EDC can yield N-acylurea[24] as a stable side product that cannot revert to the precursor state, or the waste product 1-[3-(Dimethylamino)propyl]-3-ethylurea (EDU) interferes with the assembly process. We only observed minimal amounts of the N-acylurea by FTIR after three cycles (Figure SI9). In contrast, we found that addition of EDU affected the cycle drastically, which would explain the fatigue after three cycles (Figure SI10). Performing the experiment under argon to limit SiNC oxidation did not change the fatigue (Figure SI11).

From these experiments, we conclude that EDC induced the transient assembly of the SiNCs into clusters. The lifetime of these assemblies is tunable, and the assembly–disassembly process can be repeated several times. Encouraged by these results, we began exploring the properties of these SiNC assemblies for potential future biomedical applications. Recent work has shown that SiNCs are readily taken up by cells, likely through passive diffusion of the relatively small particles.[4,9] We wondered whether we could delay such passive uptake by the transient clustering of the SiNCs. Our rationale was that the particle clusters might not be taken up because of their large size. However, as the clusters disassemble the SiNC precursors become available for passive uptake (Figure 4a).

To test the delayed uptake of the particles, we confirmed the uptake of SiNCs by a mammalian cell line by incubating COS-7 fibroblast-like cells with the SiNCs for 9 h. In these experiments, the SiNCs were added to cells in a mixture of phosphate-buffered saline (PBS, see Supporting Information

© 2018 Wiley-VCH Verlag GmbH & Co. KGaA, Weinheim

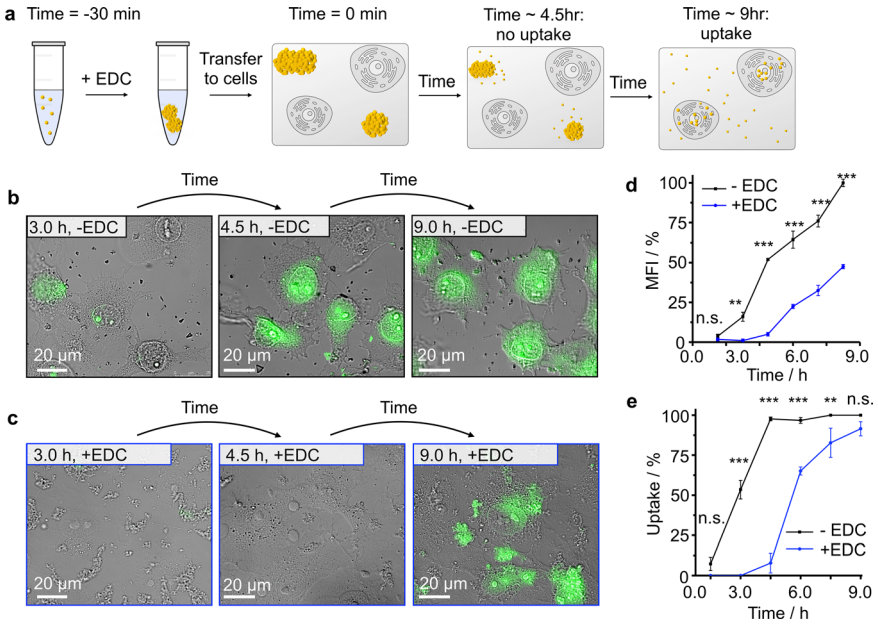

Figure 4. a) Schematic overview of the experiment. For the control experiment, no EDC is added (-EDC). The delayed uptake (4.5 h) depends on the amount of EDC added to the particles in the first step. b),c) Fluorescence micrographs of cells incubated with the SiNC solution without EDC (b) and with EDC (c) for 3.0, 4.5, and 9.0 h. d) Mean fluorescence intensity of the nucleus as a function of time for cells incubated with SiNCs and SiNCs + 9 mM EDC. The highest uptake after 9 hours is set to 100%. e) Percentage of cells that have taken up a significant amount of SiNCs, that is, with a nucleus intensity above the threshold level of 50 a.u. Error bars depict ± standard deviation of the mean for $n \geq 3$, and two-way analysis of variance (ANOVA) with a Bonferroni post-test is used between the with and without EDC at each time point. ** and *** represent a P value < 0.01 and < 0.001, respectively.

for details) and MES. At intervals of 1.5 h, the cells were thoroughly washed and tested for uptake of the SiNCs by live-cell fluorescence microscopy. We measured the mean fluorescence intensity of the nuclei of the cells. After the first 1.5 h, the mean fluorescence intensity was similar to an untreated control sample. In contrast, after 3.0 h, the cells were brighter than those of an untreated control sample (Figure 4b, Figures SI13,14). Moreover, the fluorescence intensity continued to increase with increasing incubation time (Figure 4d). To quantify the fraction of cells that had taken up SiNCs, we set a threshold value fluorescence intensity (see Supporting Information). Above this value, we considered the cell had taken up a significant amount of SiNCs (Figure 4e). The quantification of the uptake followed a similar trend over time: In the first 1.5 h, only a small fraction of the cells had taken up particles, whereas all cells had taken up after 4.5 h.

In a second experiment, the uptake of the SiNCs fueled by EDC was tested. The assembly of SiNCs was initiated by the addition of 9 mM EDC. After 30 min, the turbid solution with the SiNC clusters was added to the cells. It should be clarified that after 30 min, most of the EDC had reacted (Figure 2) and the cells were thus only exposed to minimal amounts of EDC. The lack of EDC after 30 min also implies that the growth of the clusters is likely minimal and the material properties are dominated by the hydrolysis and disassembly kinetics. We determined the lifetime of the metastable clusters to be 6 h in the presence of cell media but in the absence of cells (Figure SI15). In the first hours of the experiment with cells, we did not observe an increase in the mean fluorescence intensity of the cells (Figure 4d). Only after 6 h, did we start to see an increase in fluorescence of the nuclei compared to the control without SiNCs. Moreover, the fraction of cells that had taken up SiNCs had also drastically increased compared to earlier time points (Figure 4e). The mean fluorescence of the cells continued to increase with time, and the number of cells that had taken up SiNCs reached greater than 90% after 9.0 h of incubation. We also confirmed the viability of the COS-7 cells in the conditions we used in these experiments (Figure SI12). Finally, we confirmed the observed differences in uptake profile were not a result of the EDU, the waste product of the reaction cycle (Figure SI16).

When we compare the evolution of the uptake by the cells of the SiNC treated or not treated with EDC, a picture emerges that confirms our hypothesis. It becomes apparent that the cells cannot take up the clusters, because after 4.5 h there was an insignificant uptake when EDC was added, whereas all cells had taken up SiNCs in the experiment without EDC. This comparison points to inhibition of uptake when the SiNCs are assembled into a cluster. After 6.0 h, that is, when the clusters are disassembling (Figure SI15), we observed uptake of the SiNCs, which points to a mechanism in which the cells take up the SiNCs that have been released from the clusters. Because of the dissipative chemistry, this release of the SiNCs is delayed and so is the uptake. The fraction of cells with particles reaches similar levels as the experiments without EDC only after 9.0 h.

In conclusion, we demonstrated the dissipative self-assembly of SiNCs driven by EDC as chemical fuel. The SiNCs assembled into clusters of tens of micrometers. By varying the amount of EDC, we tuned the lifetime of SiNC clusters between 4 h and 2 days. A biological application of the transient character of SiNC clusters was explored. We showed that the time of uptake of the SiNCs by COS-7 cells could be delayed with our dissipative self-assembled system. We foresee that such dissipative supramolecular materials, whether SiNCs or other types of nanoparticles, could be used in the future to engineer materials that can delay the delivery of therapeutics into or inside cells.

Acknowledgements

This work was supported by the Technische Universität München—Institute for Advanced Study, funded by the

 © 2018 Wiley-VCH Verlag GmbH & Co. KGaA, Weinheim

These are not the final page numbers!

German Excellence Initiative and the European Union Seventh Framework Programme under grant agreement N° 291763 and the International Research Training Group ATUMS (IRTG 2022). A.A. acknowledges funding from Studienstiftung des deutschen Volkes. M.T.-S. acknowledges the European Union's Horizon 2020 Research and Innovation program for the Marie Sklodowska Curie Fellowship under grant agreement N° 747007.

Conflict of interest

The authors declare no conflict of interest.

Keywords: cellular uptake · chemical reaction network · dissipative self-assembly · non-equilibrium self-assembly · silicon nanocrystals

[1] M. Dasog, J. Kehrle, B. Rieger, J. G. C. Veinot, *Angew. Chem. Int. Ed.* **2016**, *55*, 2322; *Angew. Chem.* **2016**, *128*, 2366.
[2] a) C. M. Hessel, D. Reid, M. G. Panthani, M. R. Rasch, B. W. Goodfellow, J. Wei, H. Fujii, V. Akhavan, B. A. Korgel, *Chem. Mater.* **2012**, *24*, 393; b) O. Wolf, M. Dasog, Z. Yang, I. Balberg, J. G. C. Veinot, O. Millo, *Nano Lett.* **2013**, *13*, 2516.
[3] a) Q. Wang, Y. Bao, X. Zhang, P. R. Coxon, U. A. Jayasooriya, Y. Chao, *Adv. Healthcare Mater.* **2012**, *1*, 189; b) X. Cheng, S. B. Lowe, P. J. Reece, J. J. Gooding, *Chem. Soc. Rev.* **2014**, *43*, 2680; c) N. H. Alsharif, C. E. M. Berger, S. S. Varanasi, Y. Chao, B. R. Horrocks, H. K. Datta, *Small* **2009**, *5*, 221.
[4] F. Erogbogbo, K.-T. Yong, I. Roy, G. Xu, P. N. Prasad, M. T. Swihart, *ACS Nano* **2008**, *2*, 873.
[5] H. Nishimura, K. Ritchie, R. S. Kasai, M. Goto, N. Morone, H. Sugimura, K. Tanaka, I. Sase, A. Yoshimura, Y. Nakano et al., *J. Cell. Biol.* **2013**, *202*, 967.
[6] C. M. Gonzalez, M. Iqbal, M. Dasog, D. G. Piercey, R. Lockwood, T. M. Klapötke, J. G. C. Veinot, *Nanoscale* **2014**, *6*, 2608.
[7] a) F. Maier-Flaig, J. Rinck, M. Stephan, T. Bocksrocker, M. Bruns, C. Kübel, A. K. Powell, G. A. Ozin, U. Lemmer, *Nano Lett.* **2013**, *13*, 475; b) A. Angı, M. T. Loch, R. Sinelnikov, J. Veinot, M. Becherer, P. Lugli, B. Rieger, *Nanoscale* **2018**, *10*, 10337.
[8] M. Dutta, L. Thirugnanam, P. van Trinh, N. Fukata, *ACS Nano* **2015**, *9*, 6891.
[9] J. H. Warner, A. Hoshino, K. Yamamoto, R. D. Tilley, *Angew. Chem. Int. Ed.* **2005**, *44*, 4550; *Angew. Chem.* **2005**, *117*, 4626.
[10] B. F. P. McVey, R. D. Tilley, *Acc. Chem. Res.* **2014**, *47*, 3045.
[11] K. Dohnalová, T. Gregorkiewicz, K. Kůsová, *J. Phys. Condens. Matter* **2014**, *26*, 173201.
[12] a) S. Bhattacharjee, I. M. C. M. Rietjens, M. P. Singh, T. M. Atkins, T. K. Purkait, Z. Xu, S. Regli, A. Shukaliak, R. J. Clark, B. S. Mitchell et al., *Nanoscale* **2013**, *5*, 4870; b) A. Shiohara, S. Hanada, S. Prabakar, K. Fujioka, T. H. Lim, K. Yamamoto, P. T. Northcote, R. D. Tilley, *J. Am. Chem. Soc.* **2010**, *132*, 248.
[13] M. A. Islam, M. H. Mobarok, R. Sinelnikov, T. K. Purkait, J. G. C. Veinot, *Langmuir* **2017**, *33*, 8766.
[14] a) A. Angi, R. Sinelnikov, A. Meldrum, J. G. C. Veinot, I. Balberg, D. Azulay, O. Millo, B. Rieger, *Nanoscale* **2016**, *8*, 7849; b) M. Dasog, G. B. De los Reyes, L. V. Titova, F. A. Hegmann, J. G. C. Veinot, *ACS Nano* **2014**, *8*, 9636.
[15] a) S. A. P. van Rossum, M. Tena-Solsona, J. H. van Esch, R. Eelkema, J. Boekhoven, *Chem. Soc. Rev.* **2017**, *46*, 5519; b) A. Sorrenti, J. Leira-Iglesias, A. J. Markvoort, T. F. A. de Greef, T. M. Hermans, *Chem. Soc. Rev.* **2017**, *46*, 5476; c) R. Merindol, A. Walther, *Chem. Soc. Rev.* **2017**, *46*, 5588; d) F. Della Sala, S. Neri, S. Maiti, J. L.-Y. Chen, L. J. Prins, *Curr. Opin. Biotechnol.* **2017**, *46*, 27; e) R. Grötsch, J. Boekhoven, *Unique properties of Supramolecular Biomaterials through Non-equilibrium Self-assembly in Self-assembling Biomaterials*, Woodhead Publishing, Oxford, **2018**; f) B. Rieß, J. Boekhoven, *ChemNanoMat* **2018**, https://doi.org/10.1002/cnma.201800169.
[16] S. Maiti, I. Fortunati, C. Ferrante, P. Scrimin, L. J. Prins, *Nat. Chem.* **2016**, *8*, 725.
[17] a) J. Boekhoven, W. E. Hendriksen, G. J. M. Koper, R. Eelkema, J. H. van Esch, *Science* **2015**, *349*, 1075; b) J. Boekhoven, A. M. Brizard, K. N. K. Kowlgi, G. J. M. Koper, R. Eelkema, J. H. van Esch, *Angew. Chem. Int. Ed.* **2010**, *49*, 4825; *Angew. Chem.* **2010**, *122*, 4935.
[18] a) M. Tena-Solsona, B. Rieß, R. K. Grötsch, F. C. Löhrer, C. Wanzke, B. Käsdorf, A. R. Bausch, P. Müller-Buschbaum, O. Lieleg, J. Boekhoven, *Nat. Commun.* **2017**, *8*, 15895; b) B. Rieß, C. Wanzke, M. Tena-Solsona, R. K. Grötsch, C. Maity, J. Boekhoven, *Soft Matter* **2018**, *14*, 4852.
[19] a) A. Sorrenti, J. Leira-Iglesias, A. Sato, T. M. Hermans, *Nat. Commun.* **2017**, *8*, 15899; b) C. G. Pappas, I. R. Sasselli, R. V. Ulijn, *Angew. Chem. Int. Ed.* **2015**, *54*, 8119; *Angew. Chem.* **2015**, *127*, 8237.
[20] B. G. P. van Ravensteijn, W. E. Hendriksen, R. Eelkema, J. H. van Esch, W. K. Kegel, *J. Am. Chem. Soc.* **2017**, *139*, 9763.
[21] R. Klajn, P. J. Wesson, K. J. M. Bishop, B. A. Grzybowski, *Angew. Chem. Int. Ed.* **2009**, *48*, 7035; *Angew. Chem.* **2009**, *121*, 7169.
[22] L. Heinen, A. Walther, *Chem. Sci.* **2017**, *8*, 4100.
[23] K. A. Totaro, X. Liao, K. Bhattacharya, J. I. Finneman, J. B. Sperry, M. A. Massa, J. Thorn, S. V. Ho, B. L. Pentelute, *Bioconjugate Chem.* **2016**, *27*, 994.
[24] S. Sam, L. Touahir, J. Salvador Andresa, P. Allongue, J.-N. Chazalviel, A. C. Gouget-Laemmel, C. Henry de Villeneuve, A. Moraillon, F. Ozanam, N. Gabouze et al., *Langmuir* **2010**, *26*, 809.
[25] C. Wang, Q. Yan, H.-B. Liu, X.-H. Zhou, S.-J. Xiao, *Langmuir* **2011**, *27*, 12058.

Manuscript received: July 11, 2018
Accepted manuscript online: July 24, 2018
Version of record online: ■■ ■■, ■■■■

 © 2018 Wiley-VCH Verlag GmbH & Co. KGaA, Weinheim

Communications

Self-Assembly

R. K. Grötsch, A. Angı, Y. G. Mideksa, C. Wanzke, M. Tena-Solsona, M. J. Feige, B. Rieger, J. Boekhoven* ____ ▮▮▮▮–▮▮▮▮

Dissipative Self-Assembly of Photoluminescent Silicon Nanocrystals

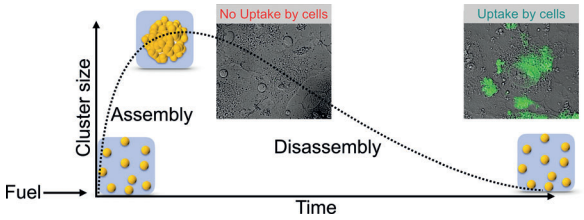

Come together: The dissipative self-assembly of silicon nanocrystals (SiNCs) is coupled to a fuel-driven chemical reaction network, thereby enabling kinetic control over the self-assembled structures. For example, the amount of fuel determines the lifetime of the assemblies. Using this mechanism, the uptake of SiNCs by cells could be delayed.

 © 2018 Wiley-VCH Verlag GmbH & Co. KGaA, Weinheim

These are not the final page numbers!